university of groningen

faculty of science and engineering

biomedical engineering

Spatial Resolution measurement on Ultra-Low dose CT image in a long axial field of view PET-CT scanner

Tygo Hillen

S4350561

Department of Nuclear medicine and molecular imaging

Period: 17/04/2023 - 01/07/2023

Bachelor's project

1st Examiner: Prof. dr. ic. C. Tsoumpas, Quantification in Molecular Diagnostics & Radionuclide Therapy, Department of Nuclear Medicine and Molecular Imaging UMCG

2nd Examiner: dr. A.T.M. Willemsen, Department of Nuclear medicine and molecular imaging

Abstract
PET-CT imaging is useful for various reasons in oncology or in other departments. However, a patient is exposed to a certain amount of dose during every scan from both the PET scan and the CT scan. This dose can have negative effects on the health of a patient in the long term and should therefore be minimised as much as possible. This study investigates the spatial resolution of an Ultra Low Dose scanning protocol. This protocol is created by adding a tin filter, reducing the current and increasing the pitch. The effect of this protocol on the spatial resolution is assessed and compared to the routine protocol used currently. To investigate this a catphan 600 phantom was used to evaluate the spatial resolution both in-plane (X, Y) and cross-plane(Z).

Before the spatial resolution could be assessed a noise reduction technique was applied called averaging. The spatial resolution was assessed with different methods to be compared with each other as well. A Point Spread Function was used besides a Slice Sensitivity Profile and an MTF. The results showed that the spatial resolution cross-plane reduced by 0.5 mm to 1.5 mm. In the X,Y plane the spatial resolution is reduced by 0 mm to 1 mm, this claim however still requires more investigation to prove.

Introduction

PET-CT imaging

A Positron Emission Tomography (PET) scan is an imaging technique used to create images of the body that show function within the body. A PET-scan is mainly used to detect tumours in different parts of the body. It is used for lung cancers (Ambrosini et al., 2012), brain cancers (Verger et al., 2022) and other types of cancer all over the body (Shukla & Kumar, 2006). PET scans can assist in diagnosing different cancers while also seeing how it is spreading and how well treatment is working. Besides its use in oncology it is also useful for certain neurological diseases such as diagnosing dementia or evaluating movement disorders such as Parkinson's. It is also used in even more specialisations such as cardiology and psychiatry. (Anand et al., 2009).

Before a PET scan is done a radioactive tracer is injected into the patient. This radioactive tracer is used by certain tissues or organs which results in a higher concentration of that tracer in that location. For example on of the most commonly used radioactive tracers is F-Fluorodeoxyglucose (FDG). FDG is a glucose derivative meaning that tissues that use a high number of sugars will have a higher FDG concentration (Ashraf & Goyal, 2022). Because the tracer is radioactive it emits a positron that will travel a small distance until it collides with an electron. Here two photons will then be released in opposite directions (Shukla & Kumar, 2006). A PET scan has detectors that can detect these photon pairs and by collecting a lot of these coincidences it is able to make an image of the body based on its functionality unlike other imaging techniques such as Computed Tomography (CT) which only give the structure of the body.

A CT image is a series of X-ray images that are called slices. By digitally stacking these slices a 3D model of a patient or object can be made and viewed from different angles. CT has a bunch of functions such as diagnosing tumours or disorders, assisting in surgery or detecting injuries present within the body (Paula & Orlando, 2023). The signal for the image is obtained by shooting electrons at a target which will then emit X-rays through an object (Tafti & Maani, 2022). These X-rays are then absorbed by the material, but how much is dependent on the type of material. This gives bone a much brighter colour on a CT than fat tissue or air which looks darker on CT images.

A PET-CT scanner is a scanner that combines A CT scan with a PET scan. Using the functional imaging of the PET scan with the highly detailed images of CT. This is done for three reasons. The first one being the attenuation correction. A conventional PET scan is corrected with a transmission scan. If no attenuation correction is done it looks like there is more activity on the outside layer of the body and it reduces the deeper inside the body you go (Schöder et al., 2003). The CT scan is a good method to make an attenuation map which creates an image that is more accurate. The second advantage of combining CT with PET is that the CT gives some anatomical information. When the PET scan and CT scans are made, they are laid over each other creating a fused image (Sureshbabu & Mawlawi, 2005). This adds more structural information to the PET scan, see Figure 1. The third reason is that combining the two different modalities improves the diagnostic accuracy of the system.

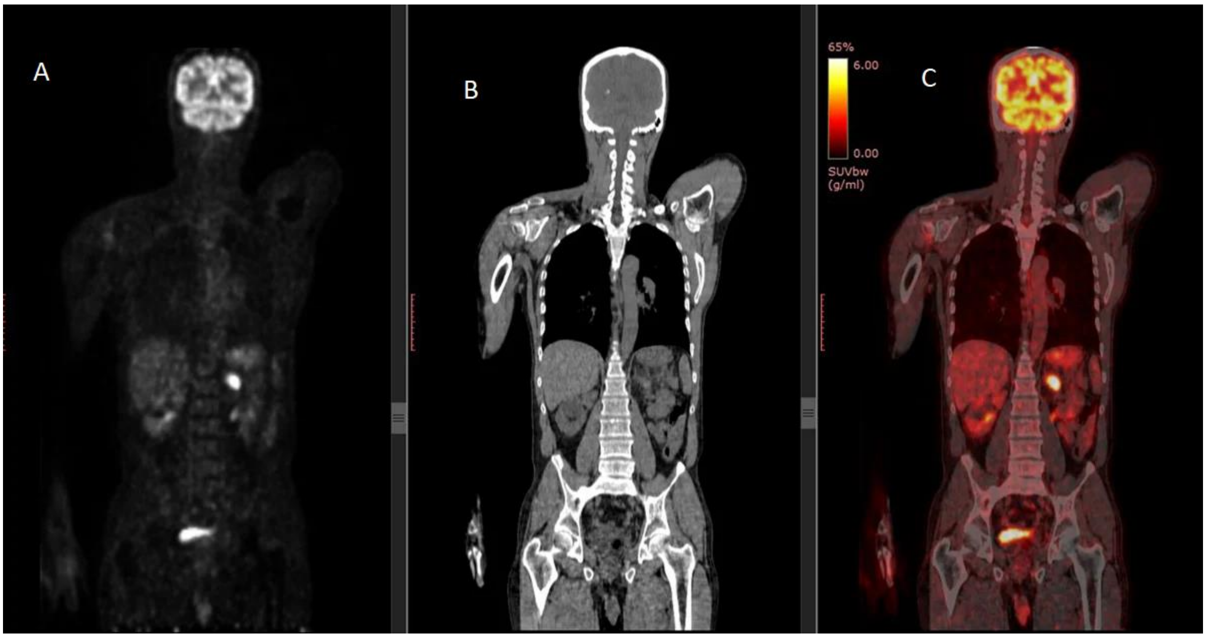

*Figure 1, A PET scan (A), A CT scan (B) and the fused image of the PET scan and the CT image (C). (*PET Scan Vs CT Scan*, n.d.)*

Dose

When performing a PET-CT scan there are two sources of radiation. The radioactive material injected into the patient for the PET scan and the X-rays created during a CT scan. It is estimated that the dose from the tracer FDG is around 7 mSv and can be up to 25 mSv for a CT scan (Akin et al., 2017). This number for the CT scan is heavily dependent on the type of scan, the duration of the scan and other parameters. For PET-CT however a non-diagnostic scan is made which has a lower radiation dose of about 7 mSv instead of the 30mSv for a whole-body high-resolution scan (Akin et al., 2017).

Even when people are not getting a scan taken, they are still exposed to other radiation coming from sources such as space or materials present on earth (Shahbazi-Gahrouei et al., 2013). This is called background radiation and in the Netherlands the background radiation is about 2.6 mSv each year for each person (*Radiation Exposure in the Netherlands | RIVM*, 2019). Meaning that if a PET-CT scan gave a total of 15 mSv it would still be almost 6 times more than the average background radiation everyone is exposed to.

Being exposed to high radiation doses brings some risks with it. When exposed to doses exceeding 30 Gy there can be severe damage to nervous tissues or other tissues. Some immediate symptoms are nausea vomiting and hypotension (Mettler & Voelz, 2002). The dose used in medical imaging is fortunately not close to these doses, but it still brings a big risk in the form of an increased risk of cancer (Redberg, 2009). De González (2009) estimated how many deaths were going to happen as a direct consequence of a CT scan. They estimated that from 72 million CT scans in the US 29.000 would later develop cancer with a 50% mortality rate. Less radiation dose would decrease the risk of cancer which is why it is one of the main objectives for improving medical imaging (Shah et al., 2012).

For reducing the dose of the PET scan the best option currently is to optimise the FDG dose and scanning time. (Akin et al., 2017).
A diagnostic CT has a high radiation dose ranging from 11-90 mSv (Akin et al., 2017), (Redberg,

2009). For a PET-CT scan these are however not necessary, and a lower dose CT is used for the fusion and the attenuation correction which ranges around 3-7 mSv (Akin et al., 2017). This is possible because the CT is not used for its high-resolution images but to create a low-resolution attenuation map. This means that the high-quality CT image is not necessary because it will be matched to the PET resolution which is worse than CT. This lower dose can be achieved by lowering the voltage, the tube current, the exposure time, increasing the pitch or by using a filter (Akin et al., 2017, McNitt-Gray, 2006).

Image Quality and spatial resolution

Medical imaging is done for a variety of reasons like diagnosing, assisting in surgery or seeing how the body is responding to treatment. To ensure these tasks can be done successfully and accurately the image needs to be of a certain quality. If a CT image does not have good enough image quality its diagnostic qualities could decrease and the scan could give false results or no results. Image quality is usually measured in three parameters: contrast, noise and resolution (Goldman, 2007).

The ability of a scanner to distinguish two different objects with a similar attenuation is called the contrast resolution. In CT the contrast resolution is worse than that of PET (Lin & Alessio, 2009). Which is why a contrast is used in a lot of CT scans. This is not necessary with a PET-CT because this has a very good contrast resolution from the tracer.

When performing a CT on a uniform object you would expect to have the whole image have the same grey scale value. In practice this is not the case and fluctuations are observed around an average (Goldman, 2007). This is called noise and is present in every image taken, see **Error! Reference source not found.**. Noise decreases the contrast resolution of a scanner, so a higher amount of noise gives a worse contrast resolution. Noise is inversely related to dose. So a higher mAs gives less noise but increases the total dose (Seeram, 2015). A filter can also be used to alter the effect of noise. A smooth filter would lessen the effect of noise but blur the image. A sharp filter would increase the effect of noise but also sharpen the edges in the image.

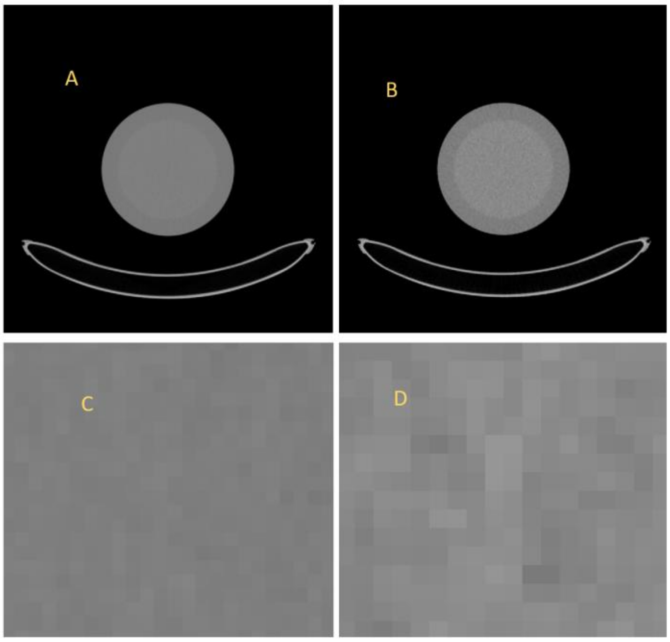

Figure 2, A) shows a slice from a routine scan. Table of the scanner is at the bottom and the circular phantom in the middle. B) Same slice as A but made with the ultra-low dose (ULD) protocol. C) Zoomed in image of a ROI of A, shows a uniform area *with similar grey values but some noise is still visible. D) Zoomed in image of B, shows a uniform area with a significant increase in noise compared to C.*

Spatial resolution is the biggest advantage of a CT scan. It describes the ability to differentiate between two tiny objects which are close together (Goldman, 2007). A higher spatial resolution means that an observer can see sharp edges of closely located objects and a low spatial resolution means that these edges get blurry and may even completely blend together. A lot of different factors can influence the spatial resolution. Some are the focal spot, detector size, a tin (Sn) filter, pixel size, pitch value, mAs and slice thickness. Some of these parameters are also related to the dose. A lower mAs would decrease the dose but might also decrease the resolution (Thunthy & Manson-Hing, 1978). A higher pitch factor would reduce the resolution of an image in the Z-plane (Lestariningsih et al., 2019) but would also decrease the dose, because of a shorter scan duration. The use of a tin filter decrease the dose by filtering out lower energies, but also increases the image quality by increasing the beam quality (Greffier et al., 2020).
Temporal resolution is the ability of a scanner to make the image of a moving object. For most CT applications this is no problem because the CT has a good temporal resolution. The only time that temporal resolution causes some problems is during a cardiac CT (Lin & Alessio, 2009).

Research question, relevance and hypothesis

The aim of this project is to evaluate the effect of an ultra-low dose CT (ULD-CT) sequence on the spatial resolution of a PET-CT scanner. Two different scan sequences will be done on a phantom and the spatial resolution in 2D and 3D is then measured. If the spatial resolution is still less than the PET scan it would be an option to choose in a clinical setting, because it would reduce the amount of dose without giving up any diagnostic capabilities of the scan since the CT scan is changed to the matrix size of the PET scan meaning the spatial resolution would decrease anyway. The spatial resolution of the CT however cannot be worse than the PET scan since it could decrease the diagnostic capabilities of the final image.
The ULD-CT is hypothesised to have an equal spatial resolution in the X, Y plane compared to the routine CT used. In the Z direction the spatial resolution would decrease but still be better than the PET resolution.

A secondary aim of this project is to compare different methods of measuring the spatial resolution. This is done to see if it gives a significant difference if a different method is chosen. It is hypothesized that the spatial resolution would be roughly the same for the different methods used, but some variation is expected.

Material and Methods

The Biograph Vision Quadra

The scanner used during this study is the biograph vision quadra. This is a PET-CT scanner made by Siemens. This specific scanner has a Field of View (FOV) of 106 cm. This is significantly more than the conventional FOV which is between 15 cm and 25 cm. This big FOV allows a patient to be scanned from their head to their thighs without moving the bed. This gives a wide range of advantages from addressing currently unsolved medical problems to reducing the amount of injected tracer (Katal et al., 2022). This scanner gives the option to use an ultra-low dose (ULD) CT scanning routine. This uses a filter and changes some other parameters.

The Catphan 600 Phantom

The phantom used for this study is the Catphan 600. This phantom is used for two different modules: CTP528 and CTP401. CTP401 contains is a set of wires angled at 23 degrees that can be used for an indirect measurement of the spatial resolution in the Z direction. CTP528 is useful for two reasons. The first one is a set of beads present within a uniform area. This can be used to calculate the spatial resolution in the X, Y direction, but also in the Z direction. The other has 21-line pairs per centimetre which can be used to calculate the spatial resolution in the X, Y plane. Both modules are used to calculate the spatial resolution in different planes using different methods.

Image acquisition

Two image protocols were created and are further detailed below. The Routine protocol was repeated 5 times and the ULD protocol was repeated 38 times.

Routine protocol

The Routine protocol had a slice thickness of 1.5 mm. The peak kilo voltage (kVp) output was 80 kV and the current in the X-ray tube was 47 mA. The focal spot was 0.9 mm and the pitch factor was 1.1 The matrix was 512x512 with a pixel spacing of 0.9765625 in both X and Y direction. The total effective exposure (McKenney et al., 2014) was 14 mAs.

ULD protocol

In the ULD protocol some of the parameters did not change compared to the routine protocol. The slice thickness is still 1.5 mm, the focal spot is still 0.9 mm and the matrix and pixel spacing are the same size. For both reconstruction protocols the bf37f kernel was used. The scanning parameters that did change were the kVp that increased to 100 kV, the tube current that decreased to 20 and the pitch factor that increased to 1.7. This causes the effective exposure to be 5 mAs. In this protocol a tin filter was also used instead of no filter.

Spatial resolution measurements

Point Spread Function (PSF)

Using the single beads in the CTP528 module a PSF can be estimated of the scan. An example of a PSF is visible in **Error! Reference source not found.**. By adding together the values of the pixels in each column a Line Spread Function (LSF) can be obtained. Obtaining the Full Width Half Maximum from this LSF data gives an indication for the Spatial Resolution.

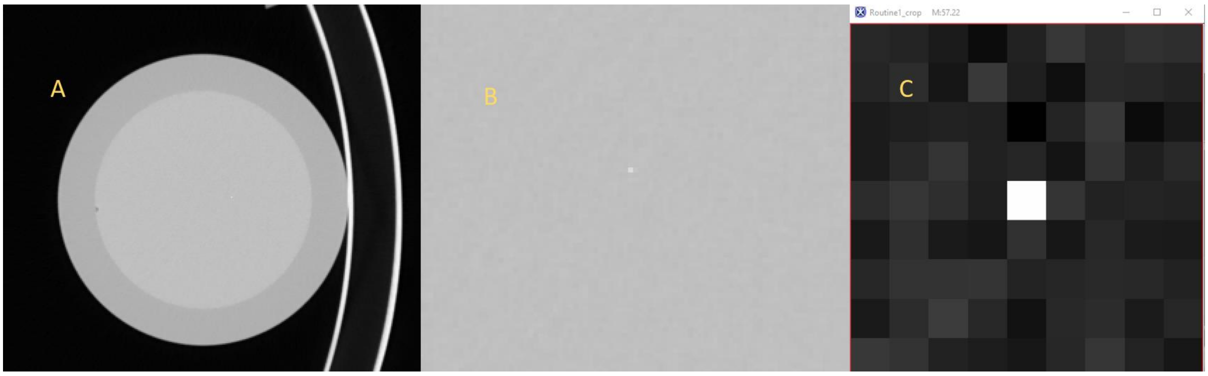

Figure 3, A) Image of a routine protocol scan of a slice containing the bead used as a PSF. B) Zoomed into the images making the bead visible. C) The pixels around the bead are now clearly visible and the exact location of the bead could even be determined.

Slice Sensitivity Profile (SSP)

The Slice sensitivity profile is similar to the point spread function. It is obtained by looking at the bead from a sagittal or coronal view, see figure 4. Here the bead will look like an ovoid object or a small line instead of a point. The FWHM from this SSP can be obtained and is a measurement for the spatial resolution in the Z direction. For calculating the SSP a zoomed in plot is made again similar to **Error! Reference source not found.**. Then the columns are added together again making sure the left-over data is the data in the Z direction. This can be plotted and used for calculating the FWHM which is an indication for the spatial resolution.

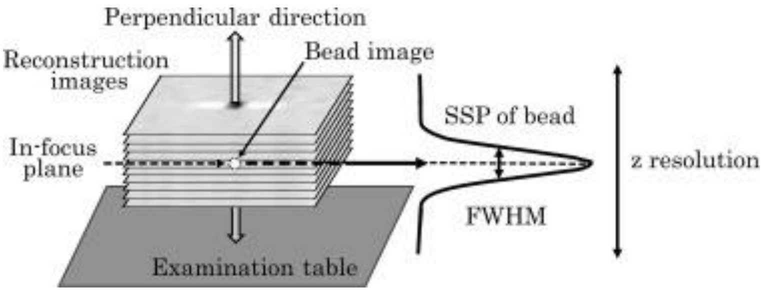

Figure 4, SSP explained. The bead is visible in the middle of the phantom and by viewing it from this angle the SSP can be obtained. This is similar to a plot profile and by getting the FWHM from this the z resolution is obtained (Kuramoto et al., 2018).

Line Pairs

The module with the 21-line pairs can be used to calculate the spatial resolution in the X, Y plane. A plot profile is made through each line pair. Using the Min and Max value <u>within</u> these line pairs and Formula 1 the MTF can be calculated. Plotting the MTF obtained at different line pairs can give an MTF plot.

MTF = (Max-Min)/(Max+Min) (Formula 1)

This MTF curve is used to assess the spatial resolution. The MTF50 is also obtained and used to evaluate the spatial resolution. This is where the mtf is at 50% of its strength.

Image J/SPICE-CT

The Dicom-viewer ImageJ has a plugin called SPICE-CT. This software has a couple of automatic programs that can be used to evaluate the spatial resolution.

First up is the MTF function. This is a function that looks for beads (in a ROI if given) and plots the MTF of this function. It also gives the MTF50, and both these things can be used to evaluate the spatial resolution.

The second function is FWHM from ROI. This software gives the FWHM from a ROI similar to what was calculated manually for the PSF and SSP. This also gives the FWHM if the ROI was around an angled wire.

The MTF function is used on the bead in the axial view calculate the spatial resolution in the X, Y plane.
The FWHM from ROI was used on the bead for the X, Y plane and on the angled wire for the Z plane.

Noise reduction/suppression

An important part in using the phantom to perform these measurements is finding the necessary components within the image. The ULD protocol gives images with a lot of noise and this can turn give some issues with finding the beads for example, see Figure 1figure 5. The noise was also too much for some of the measurements that were done. This means that the noise had an effect on the measurement of the spatial resolution, which would indicate noise has an effect on spatial resolution when it does not (McNitt-Gray, 2006).
In order to reduce the noise within the images the same image protocol is repeated multiple times and the images are then averaged (Urikura et al., 2014). The routine protocol is repeated 5 times and the ULD protocol is repeated up to 35 times. This made images with less noise which made the beads more clearly visible, see figure 6.

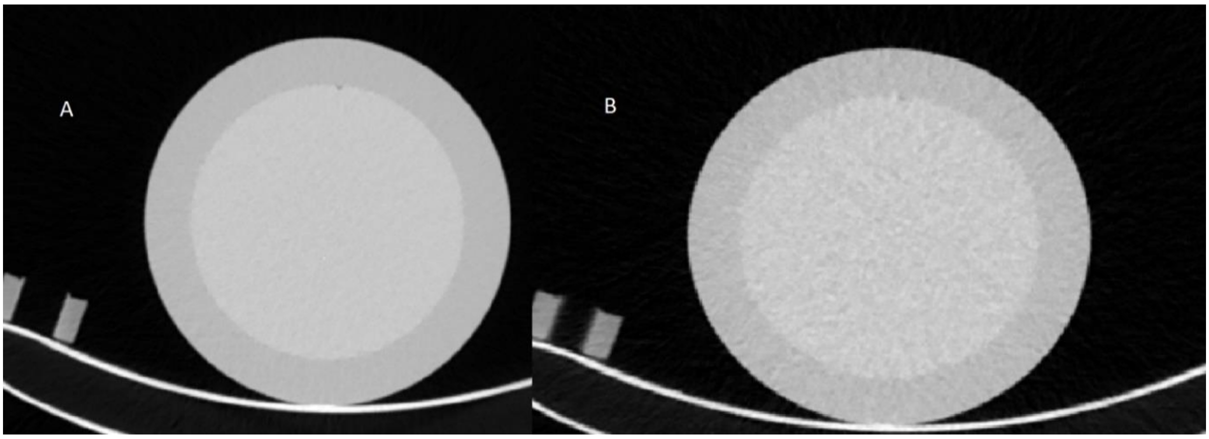

Figure 5, a single scan from the Routine protocol(A) and the ULD protocol(B). In the routine protocol a small white is visible right below the middle. This is the bead necessary for the PSF and SSP measurement. In the ULD protocol this dot is not visible

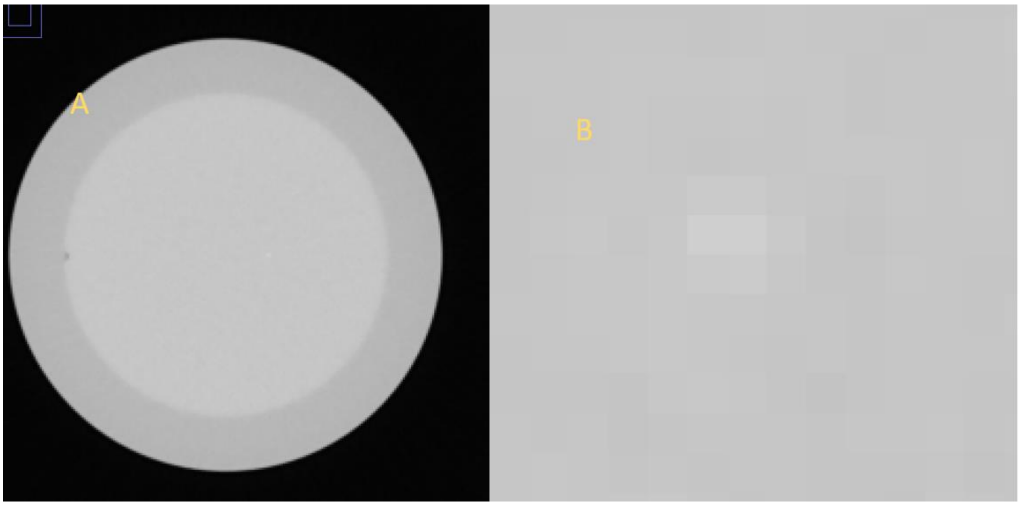

Figure 6, An image from the ULD after averaging with 38 images. A) the whole slice here the bead is barely visible. B) Zoomed in into the region containing the bead and a couple of pixels are brighter compared to the surrounding area.

Results

Results PSF

The PSF of a routine scan and a ULD scan were obtained and looked at. After inspecting a single scan it was already clear that the bead was not visible in the scan obtained from the ULD scan, see figure 7. So the Routine protocol was averaged over 5 images and the ULD protocol was averaged over 5, 10, 15, 20, 25, 30 & 35 images. After averaging the PSF looked to have improved visually.

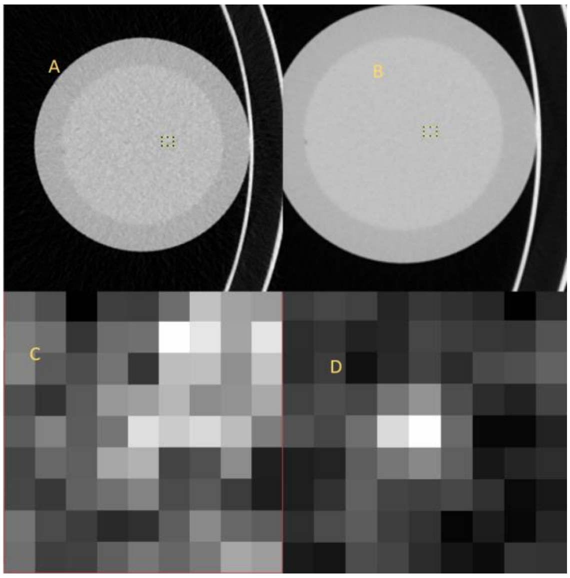

Figure 7, PSF from a ULD scan. A&C are an ULD image without averaging. The bead is not clearly visible and is expected to not give good measurements. B&D is the image after averaging over 10 images which already makes the bead more clearly visible. A and B both contain a yellow square, this is the ROI used for obtaining C&D respectively.

From all PSFs obtained the LSF was made and plotted. In figure 8 below the ULD scan is plotted and the ULD scan after averaging with 10 images is plotted. The plots of the ULD scan after averaging and the Routine protocol looked similar visually.

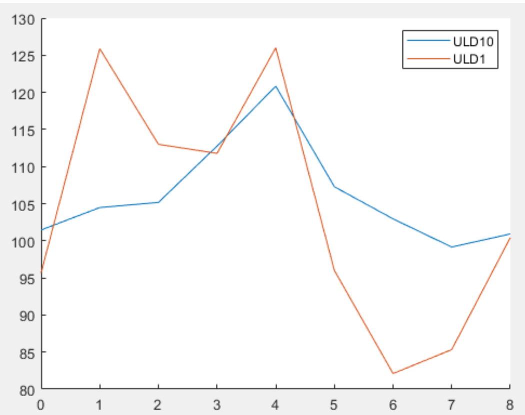

Figure 8, The LSF from the ULD scan and the LSF from the ULD scan after averaging 10 times. The peak is for both plots in the same spot and somewhat just as high. However, the scan without averaging shows a lot more variability and even has two peaks.

From the plots obtained the FWHM was calculated. For the Routine protocol this was 1.10 ± 0.07 mm after averaging with 5 images. For the ULD protocol an extra step was needed. Averaging may have helped reduce the noise in the image and made the spatial resolution measurement better, but how many images should be used for averaging. For this reason multiple amount of images was used and their spatial resolution and error margin was calculated. See figure 9 to see how the spatial resolution changed by averaging with a different number of images. It did not change much after averaging 5 times already. Therefore the amount with the lowest error was used which was 10 images.

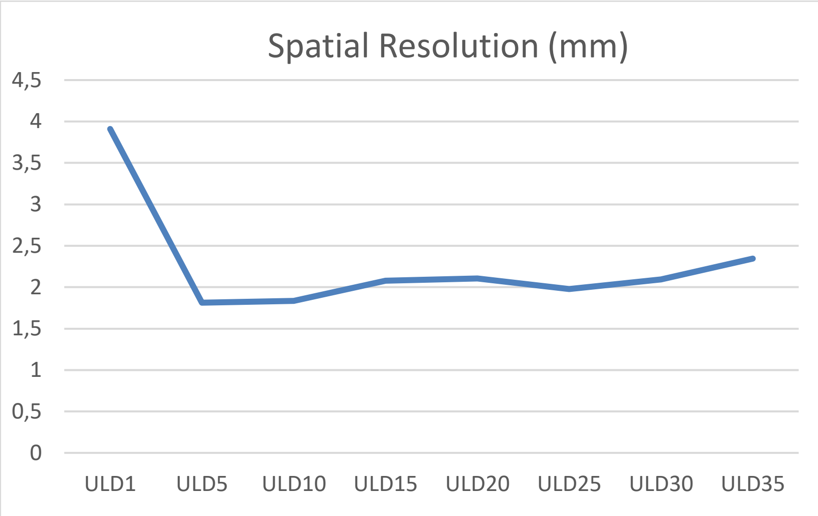

Figure 9, Plot of the effect of using more images for averaging on the spatial resolution measured from the FWHM of a LSF.

Averaging 10 times gave a spatial resolution of 2.20 ± 0.24 mm for the ULD protocol this value was obtained from the FWHM.

Results SSP

The SSP was analysed for 8 different images. Just a Routine scan, an ULD scan and 6 different ones that were averaged. 5 times for the routine protocol and the ULD protocol was averaged using 5, 10, 15, 20, 25, 30 & 35 images. The bead was viewed from the coronal plane. In figure 10 an example of a Region of Interest (ROI) is visible. Here the ovoid shape of the bead in the Z-direction is visible.

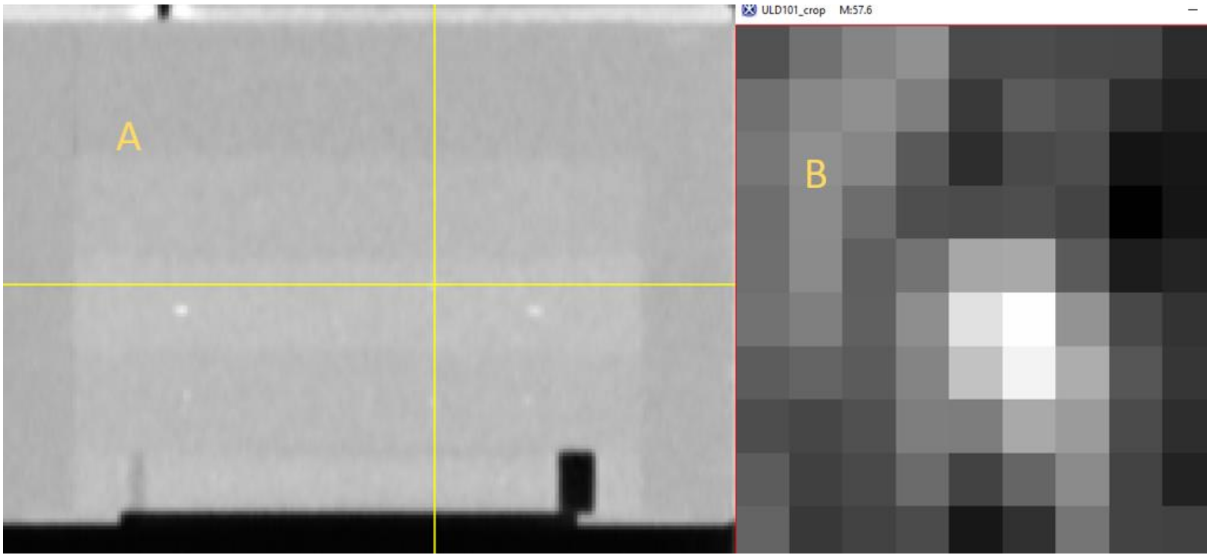

Figure 10, A) Slice containing the bead viewed in the coronal plane. Where the two yellow lines meet is the location of the bead. B) ROI of the bead viewed in the coronal plane. Image is acquired from the ULD protocol after averaging using 10 images.

The FWHM obtained from the routine protocol after averaging 5 times is 3.72 ± 0.21mm. The FWHM of the ULD protocol after averaging with 10 images is 4.72 ± 0.58 mm. The choice for using 10 images is the same as for the PSF.

Results line pairs

In figure 11 the results of the line pairs are visible. The MTF values were normalised and plotted. The Routine protocol was analysed alone and after averaging using 5 images. The same was done for the ULD but instead of 5 images 10 images were used.

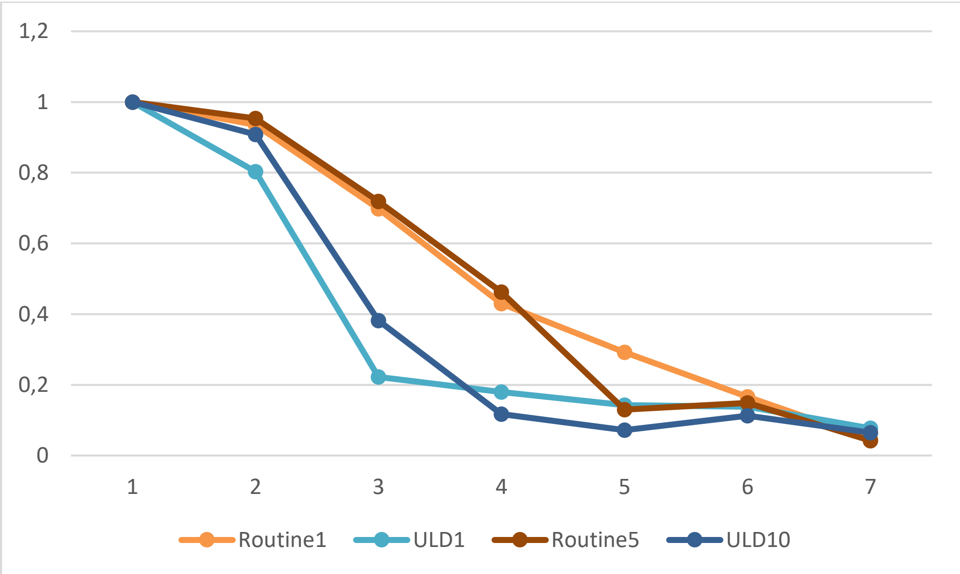

Figure 11, MTF plot for the ULD (1 and 10 images used for averaging) protocol and the Routine (1 and 5 images used) protocol. The averaging does not seem to affect the MTF that much. There is however a visual difference between the Routine and the ULD protocol.

The MTF50 is one of the ways spatial resolution is assessed. For these plots the MTF50 was 3.85 lp/cm for the routine protocol and the MTF50 for the ULD protocol was 2.78 lp/cm. This means that the ULD protocol has a lower MTF50 value and therefore has a worse spatial resolution.

Results ImageJ

In Figure 12 below the MTFs obtained from the bead in the X, Y plane are shown. These were obtained with the MTF function in the SPICE-CT plugin of the dicomviewer ImageJ. The MTF from a single ULD scan is significantly different compared to the MTF obtained after averaging. For the MTF obtained from the ULD protocol 10 images was used for averaging since this showed the lowest error.

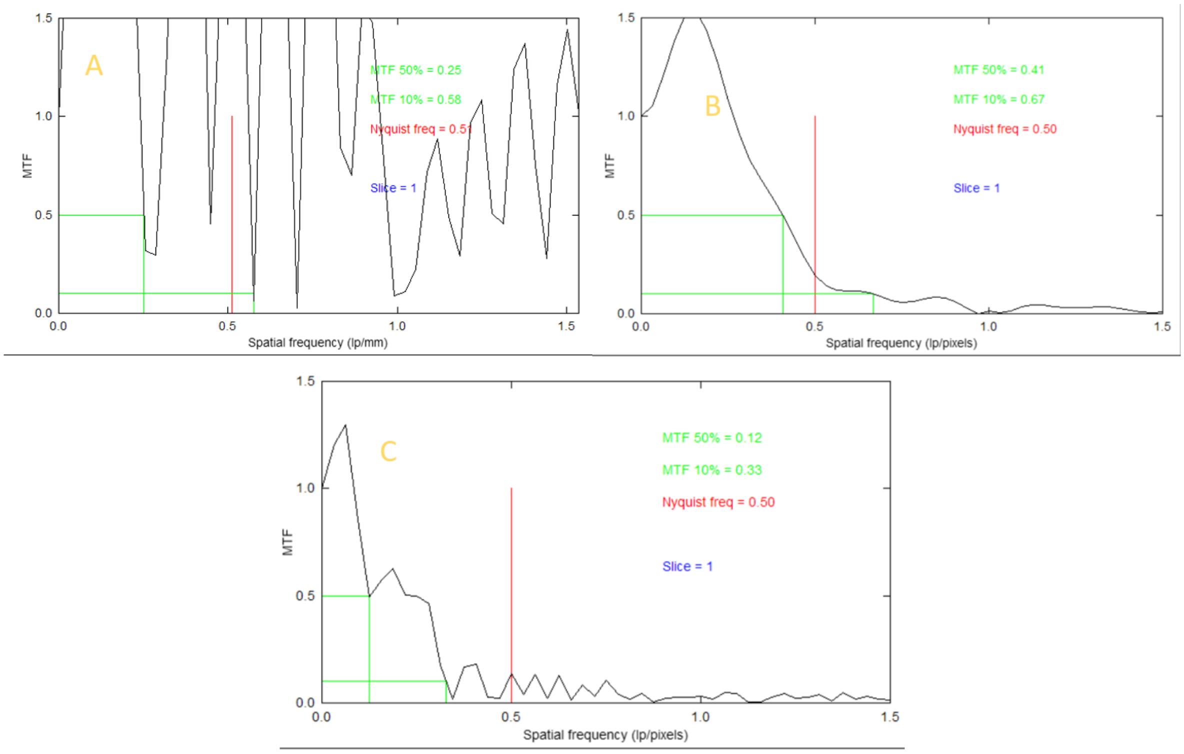

Figure 12, MTF from the ULD protocol with one scan (A) and averaged using 10 images (C). MTF from the Routine protocol after averaging with 5 images (B). All MTFs were obtained using the mtf function of the SPICE-CT plugin in ImageJ.

The MTF50 in the X, Y plane for the routine protocol was 0.34 ± 0.02 lp/mm and for the ULD protocol 0.12 ± 0.01 lp/mm.

The FWHM of ROI function within SPICE-CT was also used to evaluate the spatial resolution. In the X, Y plane this gave a FWHM for the routine protocol of 1.91 ± 0.14 mm and 2.09 ± 0.16 mm for the ULD protocol.
In the Z plane it was measured indirectly using angled wires to get 3.16 ± 0.10 mm for the routine protocol and 3.83 ± 0.10 mm for the ULD protocol.

Discussion

This study has evaluated the spatial relation of the CT scan done during a PET-CT scan for the routine protocol and for an Ultra Low Dose protocol. The ULD protocol had a higher pitch and peak kilovoltage while having a reduced tube current and it uses a tin filter. The spatial resolution was measured in different ways to evaluate different protocols for measuring the spatial resolution in both the X, Y plane and the Z plane.

Initially the noise in the images were too high for some methods of assessing the spatial resolution. This was the case for both the routine protocol and the ULD protocol, but where it was only too much a couple of times for the routine protocol it was consistently too high for the ULD protocol. This made some measurements impossible to do and put others in question during the first assessment. For example, when looking at ROIs around the bead which was used as a point spread function in an ULD scan the pixels around the bead would be consistently higher than the pixel with the bead due to the high level of noise. Getting a FWHM from this is not a good assessment for the spatial resolution. This is the reason that averaging the images was used as a method to reduce the dose. It was done to make the FWHM a more accurate indication of the spatial resolution. The averaging itself did not affect the spatial resolution but made it possible to assess it accurately. This was proven with figure 9 where the spatial resolution was measured for different images that were created using a different number of scans to average. The spatial resolution barely changed between using 5 images and 35 images but changed significantly between 1 and 5 images used. This means that the number of images used for the averaging does not affect the spatial resolution.

To see how many images would be used for averaging several things were considered. First, it should be as low as possible to make the assessment easier and quicker. It is also as low as possible to give more possible combination of images without a lot of overlap between two. What this means is that with the limited number of images that were obtained (38) not a lot of combinations can be made if the averaging is done with 35 images. Only 3 images can be swapped, but the rest are all the same making the images after averaging similar. However, using only 5 images of the 38 allows for 7 different image sets of 5 without any overlap. 5 images were however not good enough since this still gave images that were difficult to work with from time to time. This is why 10 images were used or 15 images were used. Whichever gave the lower amount of error between its image sets. For the routine protocol 5 images were used for averaging. Compared to literature 5 images and 10 images are a low number of images used. For example, Urikura et al. (2014) used 50 images and Narita and Ohkubo (2020) even used 200 images. Why these numbers were chosen is not further elaborated on. For this study the number of images used did not seem to have an influence on the spatial resolution measured between 5 images and 35 images used. If the spatial resolution would have been affected if more were used like 200 images seems unlikely but not impossible.

The point spread function is a method used to assess the spatial resolution in the X, Y plane. From this PSF a Line Spread Function is made and plotted. Getting the FWHM from this plot is then an indication of the spatial resolution. For the routine protocol the FWHM was 1.10 ± 0.07 mm and for the ULD protocol it was 2.20 ± 0.24 mm. This shows that even in the X, Y plane the spatial resolution worsened by more than a millimetre. This was not expected as the initial assumption was that the spatial resolution in plane would be almost unaffected. Greffier et al. (2020b) found that the use of a tin filter increased the spatial resolution and recommended it for ULD protocols to improve the quality and reduce the dose. McNitt-Gray (2006) claims that none of the changed parameters affects the high contrast spatial resolution. Low contrast resolution can however be influenced by factors such as the kVp, mA and pitch factor. This research is seen as a high contrast resolution measurement due to the high difference in attenuation between the tungsten bead and the surrounding uniform material. The contrast is however not quantitatively measured so it is uncertain if this were true. This could be an explanation for the difference in in-plane spatial resolution between the routine protocol and the ULD protocol. The ULD protocol also had a bigger error margin of 0.24 mm compared to the routine with 0.07 mm. This could be explained by the fact that the routine version had only 2 images that could be compared. However, the more probable explanation is the higher amount of noise in the image even after averaging is still causing some significant error margins.

The SSP is the most conventional method of assessing the spatial resolution in the Z direction. Here a similar thing is done as in the PSF, but the point source is looked at from another angle. Here the routine protocol had a FWHM of 3.72 ± 0.21 mm and the ULD protocol had a FWHM of 4.72 ± 0.58 mm. Again the ULD protocol seems to have affected the spatial resolution negatively. This difference is expected due to the effect an increase of pitch has on the cross plane spatial resolution (McNitt-Gray, 2006) (Lestariningsih et al., 2019b).

The MTF is the most conventional method for assessing the spatial resolution in the X, Y plane. One of the methods for obtaining this MTF is using a line pair module. The MTF could then be assessed in two different ways. Visually, by seeing which graph is above which one it can be assessed that it is better. In figure 11 it is seen that the routine protocols are consistently above the ULD protocols indicating that the routine protocols have a better spatial resolution. This is on par with the PSF measurement but is against the initial assumption that the spatial resolution in the X, Y plane does not change with the ULD protocol. This could have the same explanation as mentioned before. The second method to evaluate the spatial resolution is with the MTF50. For the routine protocol it was 3.85 lp/cm and for the ULD protocol it was 2.78 lp/cm.

All previous measurements were done manually using Medical Imaging Processing, Analysis & Visualisation (MIPAV) and MatLab. The Dicomviewer ImageJ however has a plugin called SPICE-CT with build in software to assess the spatial resolution. These were also used to assess the spatial resolution. The first one was an mtf function that made a modulation transfer function using a single bead. This was attempted at first to do by hand, but these attempts were unsuccessful for various reasons. This software however was successful and managed to make MTFs and get their MTF50 values. 0.34 ± 0.02 lp/mm and for the ULD protocol 0.12 ± 0.01 lp/mm.

For the X, Y plane it was 0.34 ± 0.02 lp/mm for the routine protocol and 0.12 ± 0.01 lp/mm for the ULD protocol. The ULD seems to have a negative influence on the spatial resolution compared to the routine protocol. ImageJ was also used to get the FWHM from the PSF and the SSP. The PSF was measured directly and was 1.91 ± 0.14 mm for the routine protocol and 2.09 ± 0.16 for the ULD protocol. The SSP was calculated indirectly using the angled wires. It gave a spatial resolution of 3.16 ± 0.10 mm for the routine protocol and 3.83 ± 0.10 mm for the ULD protocol. Indicating the ULD protocol had a small impact on the cross plane spatial resolution. For the X, Y plane the FWHM values for the routine and ULD protocol were quite close and the error margins overlapped partially. Indicating that the spatial resolution may not actually change with the ULD protocol in this plane. For the Z plane it was again clear that the ULD negatively affects the image quality.

For future research the different components of the ULD protocol need to be examined separately to get a clearer image of what parameter is having which effect on the spatial resolution. So how much does the noise and spatial resolution change if only the pitch factor is changed. The same can be done for the mAs, the kVp and the tin filter.

Another component that can be investigated further is how many images were used for averaging. Even though it is expected that a higher number of images would not affect it all since 5 images gave similar results as 35 it could still be beneficial to see if this holds up at 200 images.

A few measuring methods were used and compared to measure the spatial resolution. However, there are still some methods that were not attempted during this research or were attempted but not successful for numerous reasons. The first method is calculating the modulation transfer function by using the PSF, LSF or Edge Spread Function (ESF) explained by Verdun et al. (2015). Here is explained how the PSF, LSF and ESF are related to each other by Fourier transform. These three parameters can however also be used to create the MTF separately. So a scan of a phantom containing a module for all three different functions could be beneficial.

In conclusion, a few different measurement methods were used which all gave very different numbers that were very difficult to compare. However, all measurements did point towards the same conclusion. That the ULD protocol had a negative effect on the spatial resolution in the Z plane. By how much is however still not precisely determined, but based on this data it is between 0.5 and 1.5 mm less for the ULD protocol. The spatial resolution in the X, Y plane is decreased by 0 to 1 mm, but more research is still needed on this. Most of the measurements point to the fact that it is affected, but the FWHM from ImageJ and the theory mentioned earlier say it should not be affected or less.

References

Akin, E. A., Torigian, D. A., Colletti, P. M., & Yoo, D. C. (2017). Optimizing Oncologic FDG-PET/CT Scans to Decrease Radiation Exposure. *Image Wisely*. https://www.imagewisely.org/Imaging-Modalities/Nuclear-Medicine/Optimizing-Oncologic-FDG-PETCT-Scans

Ambrosini, V., Nicolini, S., Caroli, P., Nanni, C., Massaro, A., Marzola, M. C., Rubello, D., & Fanti, S. (2012). PET/CT imaging in different types of lung cancer: An overview. *European Journal of Radiology*, *81*(5), 988–1001. https://doi.org/10.1016/j.ejrad.2011.03.020

Anand, S., Singh, H. B., & Dash, A. P. (2009). Clinical Applications of PET and PET-CT. *Medical Journal, Armed Forces India*, *65*(4), 353–358. https://doi.org/10.1016/s0377-1237(09)80099-3

Ashraf, M., & Goyal, A. (2022, September 3). *18F*. StatPearls [Internet]. Retrieved June 5, 2023, from https://www.ncbi.nlm.nih.gov/books/NBK557653/

De González, A. B. (2009). Projected Cancer Risks From Computed Tomographic Scans Performed in the United States in 2007. *Archives of Internal Medicine*, *169*(22), 2071. https://doi.org/10.1001/archinternmed.2009.440

Goldman, L. (2007). Principles of CT: Radiation Dose and Image Quality. *Journal of Nuclear Medicine Technology*, *35*(4), 213–225. https://doi.org/10.2967/jnmt.106.037846

Greffier, J., Pereira, F. L., Hamard, A., Addala, T., Beregi, J. P., & Frandon, J. (2020a). Effect of tin filter-based spectral shaping CT on image quality and radiation dose for routine use on ultralow-dose CT protocols: A phantom study. *Diagnostic and Interventional Imaging*, *101*(6), 373–381. https://doi.org/10.1016/j.diii.2020.01.002

Katal, S., Eibschutz, L. S., Saboury, B., Assadi, M., & Alavi, A. (2022). Advantages and Applications of Total-Body PET Scanning. *Diagnostics*, *12*(2), 426. https://doi.org/10.3390/diagnostics12020426

Kuramoto, T., Morishita, J., Kato, T., & Nakamura, Y. (2018). Variations in slice sensitivity profile for various height settings in tomosynthesis imaging: Phantom study. *Physica Medica*. https://doi.org/10.1016/j.ejmp.2018.08.009

Lestariningsih, I., Lubis, L. E., Nurlely, & Soejoko, D. S. (2019a). Effect of pitch on CT image quality based on SNR evaluation using in house phantom. *Journal of Physics*. https://doi.org/10.1088/1742-6596/1248/1/012027

Lin, E., & Alessio, A. M. (2009). What are the basic concepts of temporal, contrast, and spatial resolution in cardiac CT? *Journal of Cardiovascular Computed Tomography*, *3*(6), 403–408. https://doi.org/10.1016/j.jcct.2009.07.003

McKenney, S. E., Seibert, J. A., Lamba, R., & Boone, J. M. (2014). Methods for CT Automatic Exposure Control Protocol Translation Between Scanner Platforms. *Journal of the American College of Radiology*, *11*(3), 285–291. https://doi.org/10.1016/j.jacr.2013.10.014

McNitt-Gray, M. F. (2006). MO-A-ValB-01: Tradeoffs in Image Quality and Radiation Dose for CT. *Medical Physics*, *33*(6Part14), 2154–2155. https://doi.org/10.1118/1.2241390

Mettler, F. A., & Voelz, G. L. (2002). Major Radiation Exposure — What to Expect and How to Respond. *The New England Journal of Medicine*, *346*(20), 1554–1561. https://doi.org/10.1056/nejmra000365

Narita, A., & Ohkubo, M. (2020). A pitfall of using the circular-edge technique with image averaging for spatial resolution measurement in iteratively reconstructed CT images. *Journal of Applied Clinical Medical Physics*, *21*(2), 144–151. https://doi.org/10.1002/acm2.12821

Optimizing Oncologic FDG-PET/CT Scans to Decrease Radiation Exposure. (n.d.). Image Wisely. https://www.imagewisely.org/Imaging-Modalities/Nuclear-Medicine/Optimizing-Oncologic-FDG-PETCT-Scans

Paula, R. P., & Orlando, J. (2023, January 2). *CT Scan*. StatPearls. Retrieved June 5, 2023, from https://www.ncbi.nlm.nih.gov/books/NBK567796/

PET Scan Vs CT Scan. (n.d.). Neurlogica. https://www.neurologica.com/blog/pet-scan-vs-ct-scan

Radiation exposure in the Netherlands | RIVM. (2019, November 5). https://www.rivm.nl/en/radiation-exposure-in-netherlands

Redberg, R. F. (2009). Cancer Risks and Radiation Exposure From Computed Tomographic Scans. *Archives of Internal Medicine*, *169*(22), 2049. https://doi.org/10.1001/archinternmed.2009.453

Schöder, H., Erdi, Y. E., Larson, S. M., & Yeung, H. W. (2003). PET/CT: a new imaging technology in nuclear medicine. *European Journal of Nuclear Medicine and Molecular Imaging*, *30*(10), 1419–1437. https://doi.org/10.1007/s00259-003-1299-6

Seeram, E. (2015). *Computed Tomography: Physical Principles, Clinical Applications, and Quality Control*. Saunders.

Shah, D. O., Sachs, R. K., & Wilson, D. (2012). Radiation-induced cancer: a modern view. *British Journal of Radiology*, *85*(1020), e1166–e1173. https://doi.org/10.1259/bjr/25026140

Shahbazi-Gahrouei, D., Gholami, M., & Setayandeh, S. S. (2013). A review on natural background radiation. *Advanced Biomedical Research*, *2*(1), 65. https://doi.org/10.4103/2277-9175.115821

Shukla, A., & Kumar, U. (2006). Positron emission tomography: An overview. *Journal of Medical Physics*, *31*(1), 13. https://doi.org/10.4103/0971-6203.25665

Sureshbabu, W., & Mawlawi, O. (2005). PET/CT imaging artifacts. *PubMed*, *33*(3), 156–4. https://pubmed.ncbi.nlm.nih.gov/16145223

Tafti, D., & Maani, C. V. (2022, August 1). *X-Ray Production*. StatPearls. Retrieved June 5, 2023, from https://www.ncbi.nlm.nih.gov/books/NBK537046/

Thunthy, K. H., & Manson-Hing, L. (1978). Effect of mAs and kVp on resolution and on image contrast. *Oral Surgery, Oral Medicine, Oral Pathology*, *46*(3), 454–461. https://doi.org/10.1016/0030-4220(78)90414-0

Urikura, A., Ichikawa, K., Hara, T., Nishimaru, E., & Nakaya, Y. (2014). Spatial resolution measurement for iterative reconstruction by use of image-averaging techniques in computed tomography. *Radiological Physics and Technology*, *7*(2), 358–366. https://doi.org/10.1007/s12194-014-0273-2

Verdun, F. R., Racine, D., Ott, J., Tapiovaara, M., Toroi, P., Bochud, F., Veldkamp, W. J. H., Schegerer, A. A., Bouwman, R. A., Giron, I. H., Marshall, N. J., & Edyvean, S. (2015). Image quality in CT: From physical measurements to model observers. *Physica Medica*, *31*(8), 823–843. https://doi.org/10.1016/j.ejmp.2015.08.007

Verger, A., Kas, A., Darcourt, J., & Guedj, E. (2022). PET Imaging in Neuro-Oncology: An Update and Overview of a Rapidly Growing Area. *Cancers*, *14*(5), 1103.
https://doi.org/10.3390/cancers14051103